JOURNAL OF AGRICULTURAL AND FOOD CHEMISTRY

pubs.acs.org/JAFC Article

Comparisons between Myofibrillar Protein−Luteolin Conjugates Fabricated through Covalent and Noncovalent Modification

Zhenyang Wu, Xue Zhao,* and Xinglian Xu*

Cite This: J. Agric. Food Chem. 2023, 71, 9908−9921 Read Online

ACCESS | Metrics & More | Article Recommendations | Supporting Information

ABSTRACT: Protein−flavonoid conjugation is considered to effectively enhance the functionality of proteins, although how different binding modes affect the conformation and antioxidative properties of these conjugates has yet to be revealed. Herein, myofibrillar protein (MP)−luteolin (Lut) conjugates were noncovalently and covalently constructed using equivalent amounts of Lut (10.00, 20.11, and 69.60 μmol/g protein). Fluorescence quenching confirmed that hydrophobic interactions were the main forces in noncovalent MP−Lut conjugates and that the binding was entropy-driven. Liquid chromatography−tandem mass spectrometry results confirmed that Lut could be covalently grafted with MP after alkaline treatment. Proteomics analysis identified that most graft sites were located on the myosin subunits. Intriguingly, in vitro results showed that the antioxidant activity was barely affected by the MP−Lut binding modes. This work provides a theoretical basis for the application of MP−Lut noncovalent/covalent complexes as functional components.

KEYWORDS: *flavonoid protein conjugates, noncovalent modification, covalent modification, antioxidant activity*

INTRODUCTION

As the major component of meat, myofibrillar proteins (MPs) can be modified as novel meat ingredients in the food industry because of their high nutritional value, high digestibility, and low allergenicity.[1] MPs have been utilized to stabilize oil-in-water (O/W) systems and provide rich palatability for emulsion-type meat products because of their excellent emulsifying capacity and gelling ability. However, lipid oxidation is the main nonmicrobial cause of quality deterioration in traditional meat products and the reaction of unsaturated fatty acids with oxygen is inevitable. Furthermore, personalized food is attracting considerable interest in the current food market, because of the potential to meet the needs of different consumer groups. Extensive studies have established that polyphenols play a significant role in derivative functions such as anti-inflammatory, antiatherogenic, antithrombotic, antimicrobial, and other bioactivities.[2,3] Natural phenolic compounds, such as propyl gallate, quercetin, catechin, and (−)-epigallocatechin-3-gallate, can interact with MPs to form MP−polyphenol complexes to prevent lipid oxidation and improve the quality and value of products.[4,5] Animal models and clinical studies have also shown that polyphenols may have a protective effect on various pathological conditions in humans.[6,7] The preparation of the MP−polyphenol complex can not only meet the demands of functional meat products and prolong the shelf-life but also has a considerable potential in developing personalized food.

Previous studies[8−10] reported that phenolic compounds including phenolic acids, flavonoids, and flavanones have a positive effect on improving the protein functional properties, such as solubility, foaming, gelling, and emulsifying. As a phenolic compound, flavonoids have three carbon bridges composed of oxygen-containing heterocycles connected to two benzene rings formed by the C6−C3−C6 structure. Compared with polar phenolic acid compounds (e.g., caffeic acid and gallic acid), flavonoids are often less soluble in polar solvents because of their lower polarity. As previously reported,[11,12] lipid oxidation in O/W emulsions mainly occurs in the biphase interface where reactive oxidation species and lipids contact. Nonpolar flavonoids tend to be adsorbed at the oil−water interface, whereas polar polyphenols tend to disperse in the continuous phase.[13] This implies that flavonoids could be more targeted in preventing lipid oxidation. Luteolin (Lut 3′,4′,5,7-tetrahydroxy flavone) is a natural flavonoid, which extensively exists in many plant species, such as celery, sweet bell peppers, and parsley.[7] As a natural antioxidant, Lut has shown effective anti-inflammation, antiallergy, and anticancer effects according to in vivo and in vitro studies.[14] Hayasaka et al.[7] have verified that Lut intake can participate in rat metabolism with anti-inflammatory effects in different forms and could ameliorate symptoms such as experimental colitis in mice by regulating apoptosis, autophagy, and inflammation. Although Lut is beneficial for human health and releases pleasant aromas at low concentrations, at high concentrations, Lut is highly irritating when uncombined, leading to poor palatability and irritation to the oral, cavity, and stomach.[15] Therefore, the advantages of conjugating Lut with MP include (1) eliminating the unpleasant taste of Lut while ensuring the biological activity of phenolic substances during digestion;[16]

Received: March 27, 2023
Revised: June 8, 2023
Accepted: June 8, 2023
Published: June 20, 2023

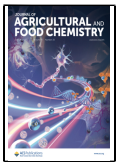

(2) increasing the solubility and bioavailability of Lut while improving antioxidant properties by using MP−Lut conjugates in the O/W system;[17] and (3) introducing Lut-fortified MP to provide an opportunity to address the growing demand for "clean label" functional meat products.[18]

The interaction between MP and phenolic compounds and their effects on MP functionalities have been extensively studied in recent years.[4,5,19] Conjugation between polyphenol compounds and proteins can be divided into irreversible binding via covalent bonds and more reversible binding via noncovalent interactions (i.e., van der Waals' forces, hydrogen bonds, and hydrophobic interactions).[20] The irreversible covalent conjugates predictably exhibit superior stability in the subsequent processing of meat products (e.g., mincing, mixing, and heating). However, covalent conjugates catalyzed by polyphenol oxidases (e.g., laccase and tyrosinase) can induce a slight decrease in polyphenol bioactivity, and the covalent conjugates produced by adding chemical reagents (e.g., glutaraldehyde) may adversely affect human health.[21] In addition, noncovalent conjugates are first choice for many researchers because of the simpler implementation method and higher feasibility in practical utilization. Nevertheless, the difference between these two modification methods on the antioxidant activity and stability of the conjugates remains unclear and the internal mechanism underlying these differences requires to be further revealed.

In this study, Lut was selected as the active flavonoid to fabricate MP−Lut conjugates. To eliminate the binding efficiency- or concentration-induced misunderstanding, samples grafted by covalent and noncovalent modifications were carefully assessed to ensure they contained an equivalent content of Lut and then the changes in MP secondary as well as tertiary structure and aggregation state were analyzed using circular dichroism, surface hydrophobicity, and sodium dodecyl sulfate-polyacrylamide gel electrophoresis (SDS-PAGE). The noncovalent modifications were explored by combining fluorescence spectroscopy with thermodynamic parameters, and mutual corroboration between MP binding sites and liquid chromatography−tandem mass spectrometry (LC−MS/MS) was used to explore the grafting sites of covalent modification. Additionally, proteomics was used to identify the proteins affected by conjugation, and particle size distribution (PSD) was used to assess changes in protein size. Finally, the effects of different modification methods on the antioxidant properties of the MP−Lut conjugate during heating were studied, which could provide valuable information in developing novel functional meat additives or products.

MATERIALS AND METHODS

Materials. The chicken breast was bought at a Suguo store, and muscle samples were bathed in ice during transportation. Luteolin was obtained from Macklin Reagent Co., Ltd. (Shanghai, China). Sodium chloride, sodium hydroxide, magnesium chloride hexahydrate, and ethylene glycol bis(2-aminoethyl ether)tetraacetate were purchased from Nanjing Chemical Reagent Co., Ltd. (Nanjing, China). All additional reagents and substances utilized in this study were at least of analytical grade.

MP Isolation. MP was extracted following the method outlined by Han et al.[22] with slight modifications. First, a quadruple volume of standard salt solution (SSS) comprising 0.1 M KCl, 20 mM K_2HPO_4/KH_2PO_4, 1 mM EGTA, and 2 mM $MgCl_2$ was combined with clipped and diced chicken breast (100 g). The mixture was then homogenized at 6700 rpm for 1 min using an emulsifier with high-purity dispersion (Prima, Model PD500-TP, England). Afterward, the above homogenate was filtered through double gauze and the filtrate was centrifuged at 2000*g* for 10 min at 4 °C (Avanti J-E, Beckman Coulter, America). The supernatant was then discarded, and the coarse MP pellet was collected to repeat the preceding procedures twice. Following that, the pellet was homogenized at 6700 rpm for 1 min with a quadruple volume of 0.1 M KCl solution, followed by centrifugation at 2500*g* for 10 min at 4 °C and then repeated once more to remove impurities and obtain pure MP. To avoid protein denaturation, all of the above procedures were carried out at 4 °C. The biuret method was used to determine the protein content of MP. The MP was used within 3 days of extraction.

Preparation of the MP−Lut Complex. The concentration of MP suspension was adjusted to 10 mg/mL with phosphate-buffered solution (PBS, 0.6 M NaCl, 50 mM K_2HPO_4/KH_2PO_4, pH 7, the same below). DMSO (dimethyl sulfoxide) was used at a concentration of 30% v/v to solubilize the Lut stock.

Covalent Modification. Covalent modification of MP with Lut was according to Ali et al.'s[23] report. Lut was initially added to MP samples (10 mg/mL, pH 7.00) at the concentrations of 15, 30, 60, 90, and 120 μmol/g protein. After fully mixing, the samples were subjected to alkaline pH shifting (pH 9 → pH 7). Briefly, the samples were adjusted to pH 9.00 with 2 M NaOH, stirred for 12 h at 25 °C with air exposure, and afterward neutralized to 7.00 with 1 M HCl.

Noncovalent Modification. Noncovalent modification of MP with Lut was according to Xu et al.'s[4] report. The MP−Lut complex was prepared by adding Lut as mentioned above; after fully mixing, the samples were incubated at 4 °C for 1 h and vortexed every 15 min. All the samples were dialyzed for 24 h at 4 °C against PBS, using an 8 to 10 kDa membrane. The unmodified protein (control) was prepared under the same conditions but without adding Lut.

Quantitation of the Amount of Lut Bound to MP. The bound Lut concentration was determined using the method described by Winters and Minchin[24] with minor modifications. By adding 1 mL of 20% trichloroacetic acid and 0.4% phosphor-tungstic acid, samples with 2 mg/mL MP were precipitated. After incubating for 30 min at 4 °C, the protein that had precipitated were washed and centrifuged at 15,000*g* for 15 min at 4 °C and then a 480 μL volume of the supernatant obtained after precipitation of protein with trichloroacetic acid was neutralized with 265 μL of 1 M NaOH. The final volume was adjusted to 500 μL and assayed for free phenol. Folin−Ciocalteu reagent was used to determine the quantity of supernatant Lut, and the standard curves of 0−2 mg/mL free Lut were measured. The bound Lut on MP was measured with the following equation:

$$\text{conjugation efficiency of Lut on MP} = \frac{\text{total amount of Lut} - \text{supernatant of Lut}}{\text{total amount of Lut}} \times 100\% \quad (1)$$

Total SH, Free SH, Free Amino, and Tyrosine Content Determination. Urea-SDS solution (8.0 M urea and 3% SDS in PBS) was used to pre-treat the MP samples (2 mg/mL), and the total sulfhydryl group (SH) was determined using the method of Xu et al.[25] by utilizing the 5,5′dithiobis-2-nitrobenzoic acid (DTNB) assay. The free sulfhydryl thiol group content in the MP samples was also determined based on the DTNB method. The content of free amino was determined using 2,4,6-trinitrobenzene sulfonic acid (TNBS) as described by Benjakul and Morrissey.[26] To compare the free amine content, the standard curve of L-leucine (in 1% SDS) was established. The content of tyrosine residues was determined according to Liu et al.[27]

Circular Dichroism (CD). After diluting to 0.05 mg/mL with PBS, the original MP and MP−Lut conjugates' secondary structural features were recorded on a J-1500 CD spectrometer (Jasco, Japan) in the range of 200−250 nm at a scan rate of 100 nm/min at 25 °C. Each sample was transferred to a 0.1 cm-path-length silica cuvette, and the PBS without adding proteins was used as the control. The spectroscopic data were analyzed to obtain the secondary structure at the online Circular Dichroism Website (http://dichroweb.cryst.bbk.ac.uk/html/home.shtml).

https://doi.org/10.1021/acs.jafc.3c01959
J. Agric. Food Chem. 2023, 71, 9908−9921

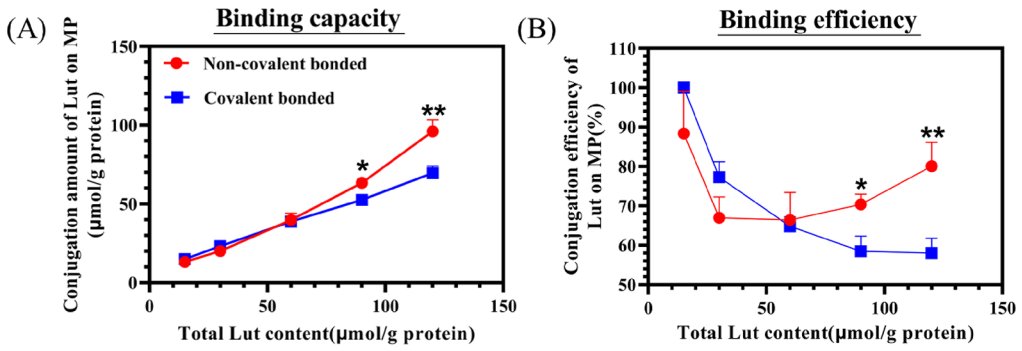

Figure 1. Impact of the various contents of Lut (15, 30,60, 90, and 120 μmol/g protein) upon noncovalent and covalent treatments on (A) the binding capacity and (B) binding efficiency of Lut on MP. *p < 0.05, **p < 0.01, ***p < 0.001 were compared between the noncovalent and covalent groups.

Surface Hydrophobicity. The surface hydrophobicity of the MP and MP−Lut conjugates was measured according to the strategies of Alizadeh-Pasdar and Li-Chan[28] with some modifications. First, PBS was utilized to dilute the samples and 4 mL of sample (1 mg/mL) was mixed with 10 μL of the fluorescence probe 8-anilino-1-naphthalene sulfonic acid (ANS) stock solution (15 mmol/L ANS in PBS). Then, the samples were kept in the dark for 20 min at an ambient temperature. A fluorescence spectrophotometer (SpectraMax M2, Molecular Devices Limited, USA) was used to determine the fluorescence. The excitation wavelength was set to 375 nm, and emission spectra were set from 300 to 500 nm, respectively; the scanning speed was 10 nm/min.

SDS-PAGE. MP and their conjugates' protein profiles were determined by SDS-PAGE. Samples (1 mg/mL) were combined with an equivalent volume of SDS-PAGE loading buffer (20% glycerol, 100 mM Tris−HCl, 4% SDS, pH 6.8) with or without 1% β-mercaptoethanol (β-ME). Dye solution (0.01% bromophenol blue) was added to the loading buffer in advance, and then all the samples were boiled for 5 min. The electrophoretic separation was run after the MP samples were loaded into the SurePAGE™ gel (4−20%, 15 wells). The gels were then stained for around 2 h using Feto SDS-PAGE staining buffer, destained overnight in deionized water, and examined using a Molecular Imager Gel Doc™ XR+ imaging system (Bio-Rad, USA). The light density value of protein bands was analyzed using ImageJ (National Institutes of Health, USA).

PSD. The PSDs were measured by dynamic light scattering (DLS) using a Zetasizer Nano ZS 90 (Malvern Instruments Ltd., Great Malvern, UK), as previously reported[29] with slight modification. The samples (0.5 mg/mL) were transferred to a quartz cuvette with a 1 cm path length and subjected to DLS measurement with a detection angle of 90° at 25.0 ± 0.1 °C.

Fluorescence Measurements. *Fluorescence Spectroscopy.* The formation of the MP−Lut conjugates was identified by the fluorescence quenching method of Dai et al.[30] with little modification. The fluorescence spectrum of the complex at 298, 308, and 318 K was recorded on a microplate reader (SpectraMax M2, Molecular Devices Limited, USA). Before measurements, the volume of samples was adjusted to 5.0 mL with PBS and then water bath, incubated at different temperatures (298, 308, and 318 K) for 40 min. The emission spectra were recorded from 300 to 500 nm, with the excitation wavelength set at 280 nm and the excitation and emission slit widths both adjusted at 2.5 nm.

Fluorescence Quenching. The interaction between MP and Lut was investigated using fluorescence quenching, and the results were evaluated using the Stern−Volmer equation:

$$\frac{F_0}{F} = 1 + K_q\tau_0[Q] = 1 + K_{sv}[Q] \quad (2)$$

where F_0 and F mean the fluorescence intensities without or with a quencher and $[Q]$ equals the quencher concentration, τ_0 ($\tau_0 = 10^{-8}$ s) is the lifetime of the fluorophore without a quencher, and K_q and K_{sv} refer to the bimolecular quenching constant and the Stern−Volmer quenching constant, respectively. The K_q and K_{sv} values are calculated by linear regression of an F_0/F vs $[Q]$ plot. Values of n (denoting the number of MP−Lut binding sites) and the equilibrium constant K_a for static quenching are calculated with the altered Stern−Volmer equation as follows:

$$\log\frac{(F_0 - F)}{F} = \log K_a + n\log[Q] \quad (3)$$

Thermodynamic Parameters and Interaction Mode. The binding properties between MP and Lut were assessed using thermodynamic parameters. The specific interaction mode between MP and Lut in the interaction process was identified using the enthalpy and entropy changes (ΔH and ΔS, respectively). The Van't Hoff equation was used to determine the values of ΔH and ΔS:

$$\ln K = -\frac{\Delta H}{RT} + \frac{\Delta S}{R} \quad (4)$$

where K is equivalent to K_a, the effective quenching constant, at the corresponding temperature. R is the gas constant [8.314 J · (mol·K)$^{-1}$]. In addition, the following formula is used to calculate the free energy variation (ΔG):

$$\Delta G = -RT\ln K = \Delta H - T\Delta S \quad (5)$$

LC−MS/MS Analysis. MP and MP−Lut conjugates' peptide after enzymolysis was separated on a Q Exactive Plus mass spectrometer coupled with EASY-nLC 1200 (Thermo Fisher Scientific). In buffer A (0.1% formic acid in water), the peptide was first loaded onto a trap column (100 μm × 20 mm, 5 μm, C18, Dr. Maisch GmbH, Ammerbuch, Germany). A self-packed column (75 μm × 150 mm; 3 μm ReproSil-Pur C18 beads, 120 Å, Dr. Maisch GmbH, Ammerbuch, Germany) was used in RP-HPLC separation using the EASY-nLC system. With a linear gradient of buffer B (0.1% formic acid in 95% acetonitrile), the dissolved peptides were eluted over the course of 120 min. A data-dependent top20 method was used to acquire MS data, dynamically selecting the most prevalent precursor ions from the survey scan (300−1800 m/z) for HCD fragmentation. For mass calibration, a lock mass of 445.120025 Da was used as the internal standard. The resolution for the full MS scans was 70,000 at m/z 200, and for MS/MS scans, it was 17,500 at m/z 200. For MS and MS/MS, 50 ms was chosen as the maximum injection time. The isolation window was set to 1.6 Th, and the normalized collision energy was 27. The dynamic exclusion lasted for 60 s. The peptides were identified by using pLabel 2.4 software to retrieve information from the corresponding database.

Antioxidant Properties. Before the measurement, all the samples were installed in centrifuge tubes and heated in the water bath at different temperatures (25, 50, and 75 °C) for 15 min. After thermal treatment, the samples were stood in an ice bath to recover to the ambient temperature. The antioxidant properties of the MP and MP−Lut conjugates were measured through 2,2-diphenyl-1-picrylhydrazyl (DPPH) and 2,2′-azino-bis (3-ethylbenzothiazoline-6-sulfonic acid)

https://doi.org/10.1021/acs.jafc.3c01959
J. Agric. Food Chem. 2023, 71, 9908−9921

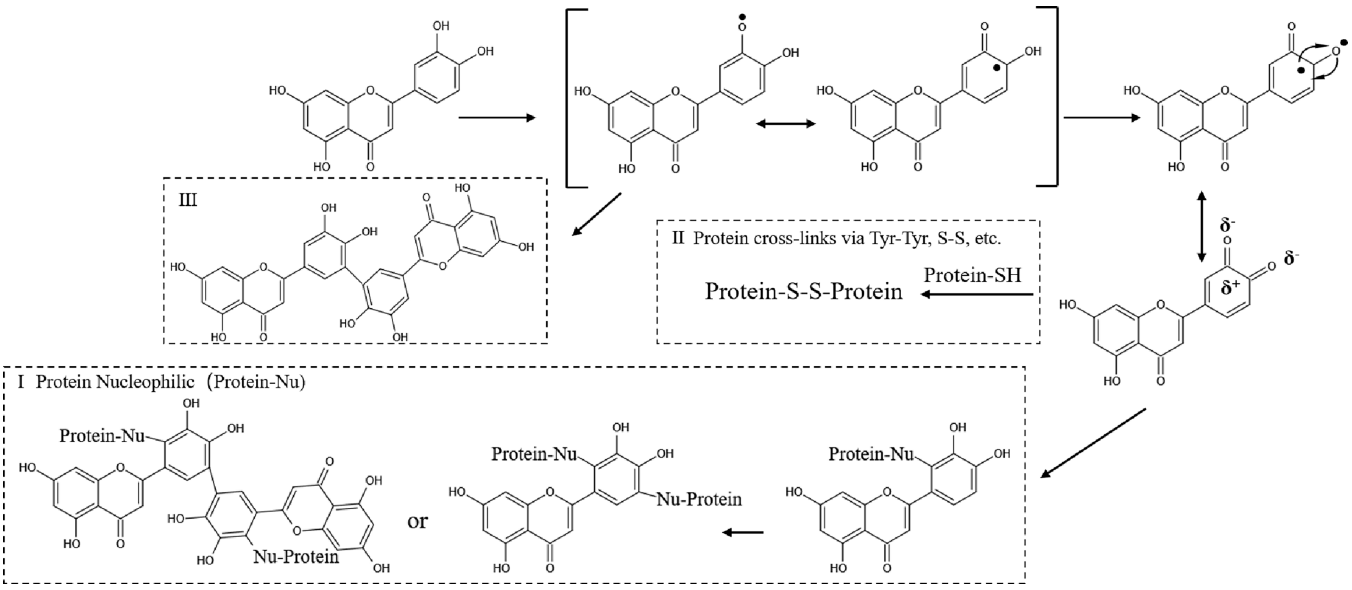

Figure 2. The summarized scheme on the oxidation of flavonoids under alkaline conditions for the formation of protein crosslinks (pathways I and II) and polymer products (pathway III) based on previous reports.[5,15,39]

(ABTS) radical scavenging activity and Fe^{2+} reducing power, which were acquired using previous strategies of Chen et al.,[19] Siddhuraju,[31] and Yıldırım et al.,[32] respectively. The ABTS scavenging activity and Fe^{2+} reducing power were calculated and expressed as μmol Trolox equivalents (TE) per g of sample based on a Trolox calibration curve, which was conducted by the strategy mentioned above.

Statistical Analysis. Each experiment involved at least three independent trials. In the analysis of variance (ANOVA), Duncan's multiple range analysis was used to determine the significant differences between the means. Statistical analysis was accomplished utilizing the SAS System for Windows V8, and the data were considered statistically significant when the p-values <0.05.

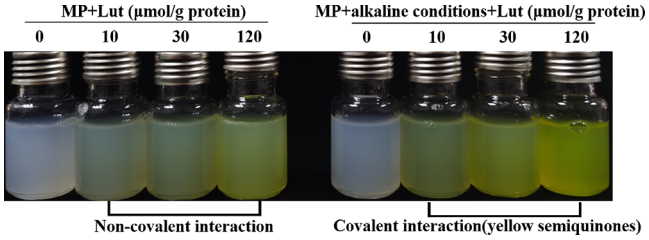

Figure 3. Effects of Lut addition (10, 30, and 120 μmol/g protein) and alkaline pH_{shift} (7.00 → 9.00 → 7.00) on color change of noncovalent and covalent-treated MP aqueous solutions.

RESULTS AND DISCUSSION

Quantitation of the Amount of Lut Bound to MP. With the gradual addition of Lut, the binding capacity of Lut increased in both the covalent and noncovalent groups (Figure 1A), indicating the successful grafting of Lut on MP molecules in different ways. Notably, the Lut binding efficiency of the covalent group decreased with the increasing Lut dose from 10 to 120 μmol/g protein, whereas the binding efficiency of the noncovalent group remained at a relatively high level, although this was lower than that of the initial value (Figure 1B). A similar phenomenon has been observed in MP−chlorogenic acid conjugates.[18] This trend of binding efficiency can be explained by the dynamic reaction equilibrium between the Lut and MPs (Figure 2). Under alkaline conditions of the covalent treatment group, the shifting between (*ortho-* or *semi-*) quinones and phenols resulted in a change of color[33] and the covalent sample accentuated the yellow color (Figure 3). For catechol-containing flavonoids, catechol groups of Lut can be oxidized into *o*-quinone by oxygen transfer and subsequent free radical formation, triggering the dimerization reaction to form biphenolic compounds (pathway III in Figure 2). The self-association of Lut via dimerization or polymerization at high concentrations may limit the binding of Lut to reactive residues of the protein, further reducing the binding efficiency of covalent groups.

To compare the physicochemical properties of covalent and noncovalent MP−Lut conjugates, it is necessary to eliminate the differences in the amount of bound Lut. MP samples covalently or noncovalently grafted with equivalent amounts of Lut were carefully obtained. Conjugates at three Lut concentrations (10, 30, and 120 μmol/g protein) were prepared by pipetting different volumes of Lut stock (360 μmol/g protein, dissolved in DMSO and mixed with PBS) into the protein suspension while vortexing. After dialyzing, the addition of 10 μmol Lut/g protein (low concentration) produced an equal binding capacity for Lut of 10 μmol Lut/g protein in both the covalent and noncovalent samples. When the addition of Lut reached 30 μmol/g protein (medium concentration), the grafting degree of noncovalent and covalent samples was 20.11and 23.19 μmol/g protein, respectively. When the addition of Lut was 120 μmol/g protein (high concentration), the substitution degree of samples in noncovalent and covalent ways was 96.12 and 69.60 μmol/g protein, respectively.

Therefore, the addition of Lut in noncovalent/covalent samples was adjusted and the final following addition content of Lut was 10.00/10.00, 30.00/24.82, and 86.89/120.00 μmol/g protein at low, medium, and high concentrations, respectively. The final total Lut contents of noncovalent and covalent MP-Lut conjugates at low, medium, and high concentrations were 10.00, 20.11, and 69.60 μmol/g protein, respectively.

MP Binding Sites. Lut (*o*-diphenols) can be oxidized into *o*-quinones, which being a reactive electrophilic intermediate

https://doi.org/10.1021/acs.jafc.3c01959
J. Agric. Food Chem. 2023, 71, 9908−9921

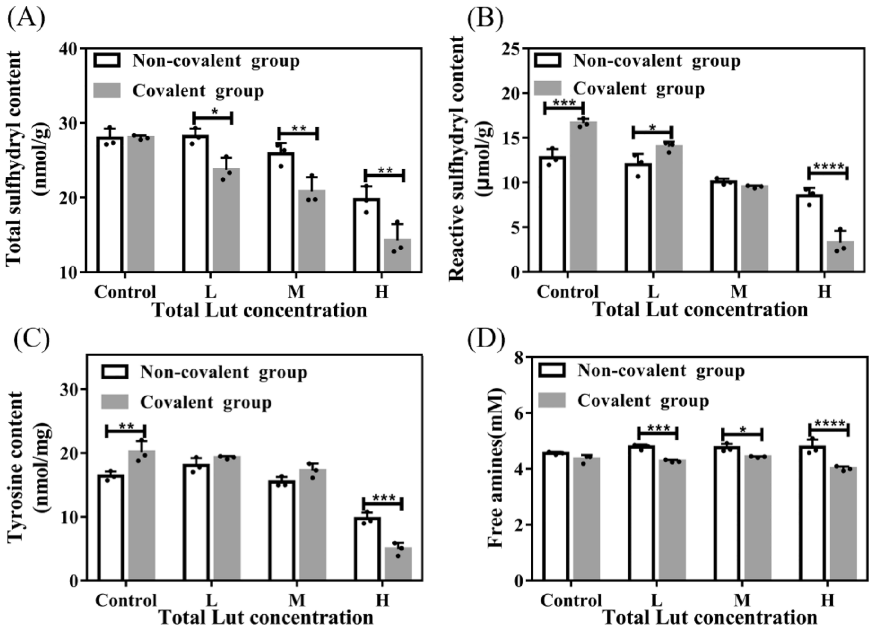

Figure 4. Impact of the various contents of Lut (10, 30, and 120 μmol/g protein) upon noncovalent or covalent treatment on (A) total sulfhydryl; (B) reactive sulfhydryl; (C) tyrosine; and (D) free amine contents of MP. *p < 0.05, **p < 0.01, ***p < 0.001 were compared between the noncovalent and covalent groups. Non-cov: noncovalent; Cov: covalent; Non-cov/Cov L, M, H: noncovalent or covalent treatments in the presence of low (L), medium (M), and high (H) concentrations of Lut (10, 30, and 120 μmol/g protein, respectively), the same below.

can react with nucleophilic groups (e.g., Lys, Cys, and Tyr residues) in MPs[15] (pathway I in Figure 2), such as lysine, tyrosine, cysteine, and tryptophan residues in a protein chain. The changes in these residues were measured to indicate a protein−phenolic interaction.[34]

Myosin (the major protein in MP) has a particularly high SH content; the amount of lost SH groups is used to sensitively assess the extent of MP oxidation. We then assessed whether the total SH content of noncovalent and covalent control MP was equal with the increase in Lut concentration. The total SH content of the noncovalent group at low and medium concentrations was not significantly different (P > 0.05), whereas the total SH content of the covalent group at these concentrations was significantly reduced (P < 0.05), causing a loss of SH of 15.27 and 25.76%, respectively. At the high Lut concentration, the total SH contents of both the noncovalent and covalent samples decreased sharply, with a loss up to 29.49 and 39.13%, respectively. This trend was similar with the changes in reactive SH content (Figure 4B), indicating that the noncovalent treatments had less effect on SH content, whereas the covalent treatment significantly reduced the content of reactive SH in a dose-dependent manner (P < 0.05), exhibiting a loss of reactive SH up to 80.42% at the high concentration (from 16.65 to 3.26 nmol/g protein in S1). The MP structure unfolded because of the covalent treatment, causing the reactive SH content in the control group to be higher than that in the noncovalent group. A comparable decline in the SH content occurred in the treatment of other MPs because of the formation of thiol−quinone adducts.[30−32] The disulfide bond (S−S) formation via the oxidation of SH groups by radicals generated by phenolic-mediated redox cycling was believed to account for the loss of these groups.[18] Thus, the total SH and reactive SH contents of covalent samples decreased at different concentrations. This could be because (1) the S−S binding was the major force in the aggregation of MP−Lut conjugates and (2) the Cys residue containing SH groups was one of the modification sites of Lut. In the noncovalent samples, (1) the presence of high concentrations of Lut may promote the oxidation of some SH groups and induce MP aggregation to a certain extent and (2) the catechol moieties of Lut may exert auto-oxidation and chemically react with the nucleophilic SH groups[35] of MP in a neutral or slightly alkaline solution (pH 7.0).

An increasing Lut concentration led to a sharp decrease in the Tyr content in both noncovalent and covalent samples (Figure 4C). The change in the Tyr content was consistent with that of SH; the noncovalent and covalent samples at high Lut concentrations caused losses of up to 40.79 and 75.52% Tyr, respectively in MP (P < 0.05). The original MP of covalently bound samples had a higher Tyr content than that of noncovalently bound MP, whereas noncovalent treatment did not significantly (P > 0.05) affect the Tyr content at the low and medium Lut concentrations. Hydrophobic interactions mainly exist between Tyr and the benzene ring of polyphenols.[36] The Tyr loss in noncovalent samples was mainly because of the direct contact between Tyr and the more polar (Lut) benzene ring at the molecular level that changed the polarity of the microenvironment near the Tyr residues.[20] For the covalent samples, this could be attributed to the reaction between oxidized Lut with MP Tyr residues and the formation of bityrosine.[34] Bityrosine production has been described as a marker for MP oxidative modification by hydroxyl radicals.[37] The Tyr content generally exhibits a positive correlation with the reactive SH content. Disulfide bridge and bityrosine formation can induce MP polymerization together. The Tyr residues thus appear to be another reactive site for Lut binding. A similar drop of the SH groups and Tyr residues in MP was also observed after reacting with catechin and gallic acid.[25]

The covalent conjugates also showed a significant (P < 0.05) but slight change in the free content of free amines compared with that in the control at the high concentration (Figure 4D),

https://doi.org/10.1021/acs.jafc.3c01959
J. Agric. Food Chem. 2023, 71, 9908−9921

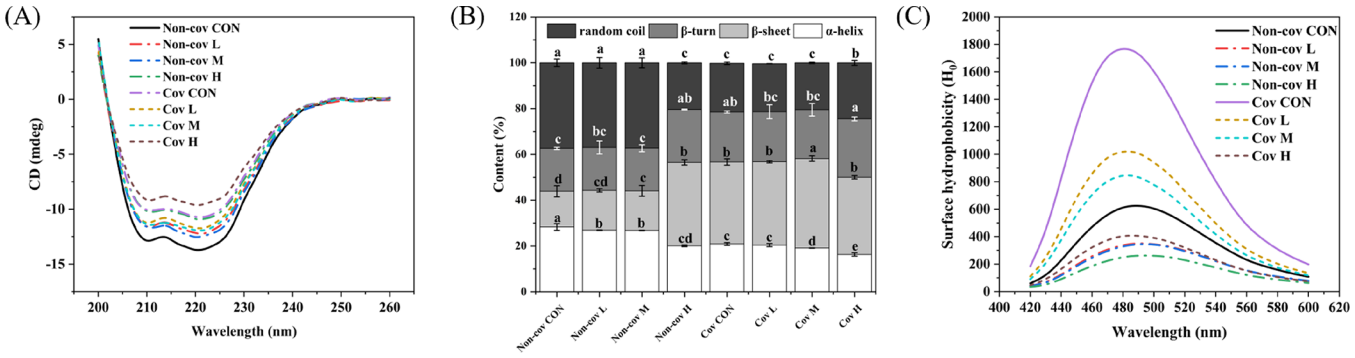

Figure 5. (A) Far-UV CD spectra; (B) the secondary structure contents; and (C) the surface hydrophobicity of MP as affected by different contents of Lut under covalent and noncovalent treatments.

which can be attributed to the reaction between Lut and Lys residues, whereas the free amine content of noncovalent/covalent samples exhibited no apparent change at other concentrations ($P > 0.05$), indicating that quinone-NH_2 adducts were not produced as a result of neutral or alkaline auto-oxidation.

These results showed that Cys, Tyr, and Lys may be the modification sites of Lut-modified MP, which was also verified in the proteomics analysis.

Structural Changes in MP. *Secondary Structure.* The CD spectrum of MP and MP−Lut conjugates revealed two negative bands near 208 and 222 nm (Figure 5A), implying the predominant presence of a-helix conformation as the myosin tail has a supercoiled α-helix structure.[38] The spectrum peaks of the different concentration samples underwent profoundly negative attenuation upon Lut addition, inferring significant losses of the α-helix structure of the MP−Lut conjugates.[18,39]

Upon covalent treatment, the α-helix structure content (Figure 5B) of the covalent control group was significantly lower than that of the noncovalent control group ($P < 0.05$). Li et al.[40] have revealed that the pH-shifting led to an MP unfolding−refolding behavior, causing the loss of an α-helix structure. Considering that the covalent samples underwent pH-shifting treatment, the α-helix content of the covalent original MP was even lower than that of the noncovalent MP. Low and medium Lut concentrations had a significant ($P < 0.05$) but minor effect on the α-helix structure content of noncovalent and covalent samples, possibly because the concentration of Lut critically promoted the MP reaction with Lut rather than affect the protein structure at low and medium doses, whereas at the high Lut concentration, the α-helix content of both the noncovalent and covalent samples decreased significantly ($P < 0.05$) accompanied by a significant increase in β-sheet and random coil content. The conjugation of flavonoids with different structures has been reported to cause the decrease in α-helix content in a variety of proteins, including MP,[18,34] egg white protein,[41] and β-lactoglobulin.[42] Our results indicated that both noncovalent/covalent binding of Lut to MP promoted the transformation of the secondary structure at the high Lut concentration, thus making the conjugate structures looser and more flexible.[25] Notably, the binding mode had a considerable influence on the protein secondary structure. The relatively higher random coil contents caused by noncovalent treatment indicated that the protein transitioned from an ordered to a disordered structure, indicating that the secondary structure of noncovalent MP−Lut conjugates was more intensely disordered than that of covalent ones.

Tertiary Structure. Surface hydrophobicity was measured to assess the influence of Lut adduction on the tertiary structure of MP. The fluorescent probe ANS combines with hydrophobic residues and elicits strong fluorescence[2] and was therefore used to evaluate the surface hydrophobicity. The surface hydrophobicity of the covalent control group was far greater than that of the noncovalent group, which indicated that the process of unfolding−refolding caused by covalent treatment exposed numerous hydrophobic residues in the MP. With the increasing Lut concentration, the surface hydrophobicity of noncovalent and covalent samples both decreased (Figure 5C), suggesting that the reaction with Lut made the surface of MP molecules more polar. Modification of oxidized phenolic compounds could also decrease the surface hydrophobicity of porcine MPs[2] and cuttlefish skin gelatin.[43] The reduction of surface hydrophobicity was mainly because the grafting of Lut blocked hydrophobic residues and thereby exposed hydrophilic regions that were previously buried.[33]

Protein Profile by SDS-PAGE. The nonreducing and reducing SDS-PAGE profiles of noncovalent and covalent samples are shown in Figure 6A and B, respectively, and the corresponding light density value changes of each lane are shown in Figure 6C,D. The reducing SDS-PAGE result exhibited a typical MP electrophoretic profile, with the major polypeptides being myosin heavy chain (MHC, 200 kDa) and actin (45 kDa). For both noncovalent and covalent conjugates, larger protein bands were present compared with the size of the control MP bands, indicating the formation of Lut-mediated MP aggregates. Large aggregates (high molecular weight aggregates, HMWA) formed concurrently and remained in the sample well while a few new bands (low molecular weight aggregates, LMWA) appeared in the protein profile at approximately 40 and 280 kDa. The highest light density value peaks of LMWA (Figure 6C, covalent H) also appeared between the peaks of HMWA and MHC bands. Generally, free radicals attack MP molecules mainly at three sites, including the backbone of peptides, aliphatic amino acid side-chain groups, and aromatic amino acid side-chain groups.[44] It can be seen from the profiles that the reaction will lead to modifications of the amino acid side chains, and the formation of intermolecular cross-linked proteins, whereas there is no peptide backbone scission or fragmentation.

The amount of Lut-induced aggregates was quantitatively related to the Lut concentration, especially at a high Lut dosage (120 μmol/g protein), which reduced the intensity of

https://doi.org/10.1021/acs.jafc.3c01959
J. Agric. Food Chem. 2023, 71, 9908−9921

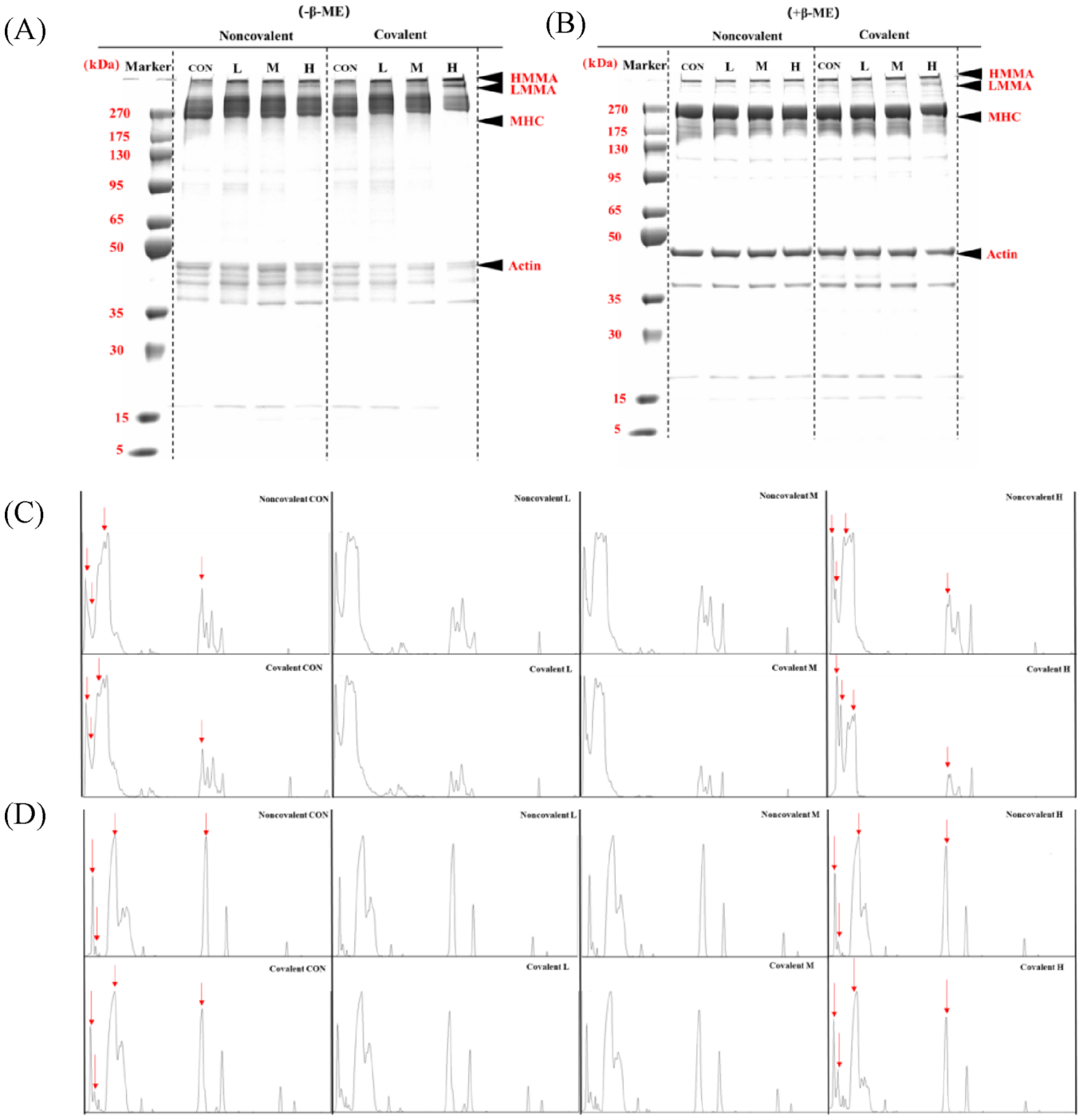

Figure 6. (A) Nonreducing and (B) reducing SDS-PAGE patterns of MP under noncovalent and covalent treatments. (C) Nonreducing and (D) reducing SDS-PAGE pattern corresponding gray value change curves. The red arrows represent HMMA, LMMA, MHC, and actin in turn. MHC: myosin heavy chain; HMMA: high molecular weight aggregates; LMMA: low molecular weight aggregates; β-ME: β-mercaptoethanol.

the MHC band and slightly reduced that of the actin bands in covalent samples. Aggregation was less apparent in the noncovalent sample bands at a relatively low dosage (10 and 30 μmol/g protein). Additionally, the light density value peaks of HMWA and LMWA in noncovalent samples (Figure 6C, noncovalent H) were lower than those of the covalent ones (Figure 6C, covalent H). Thus, more aggregates were generated through covalent treatment with the increase in Lut concentrations (pathways I and II in Figure 2), whereas the noncovalent treatments did not induce the formation of aggregates at low and medium Lut concentrations.

When compared with the reduced profiles of samples, the nonreduced profiles of samples showed higher density values for both HMWA and LMWA, suggesting that β-ME cleaved the disulfide bonds and partially diminished the amount of disulfide-linked LMWA and HMWA (Figure 6D). Conspicuous aggregates were still present, which was probably because (1) Lut acted as a crosslinker through adduction with free nucleophilic protein side-chain groups (pathway I in Figure 2) and (2) the aggregates may be cross-linked by covalent bonds other than disulfide bonds (pathway II in Figure 2), such as Tyr−Tyr and carbonyl−NH_2.[39] The Lut-dose dependent loss

https://doi.org/10.1021/acs.jafc.3c01959
J. Agric. Food Chem. 2023, 71, 9908−9921

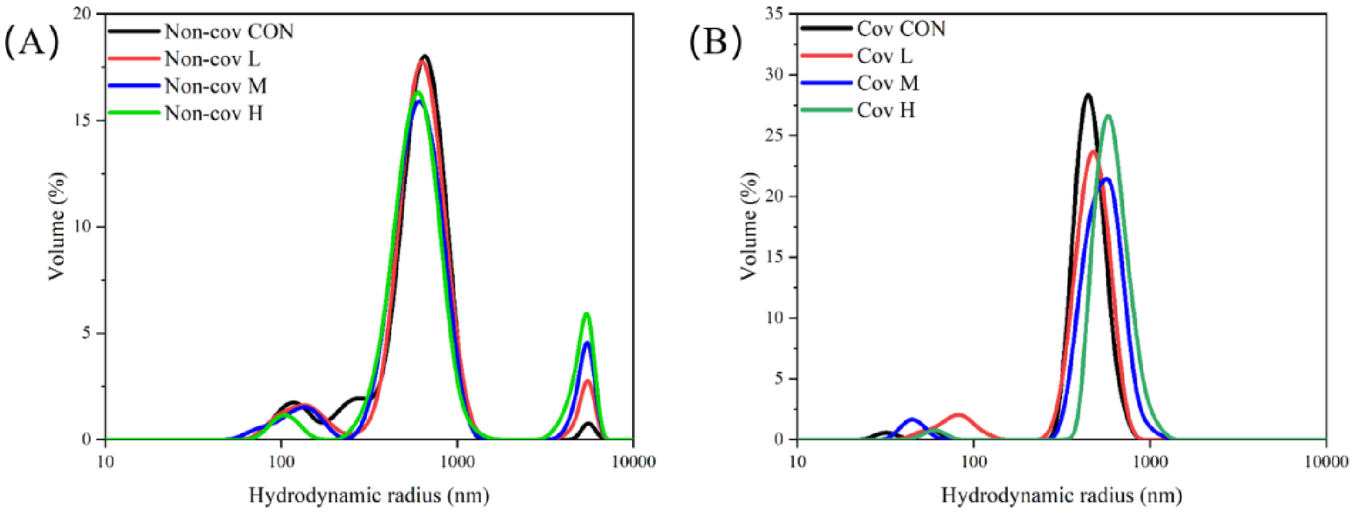

Figure 7. Particle size distribution of MP as affected by different contents of Lut under (A) noncovalent and (B) covalent treatments.

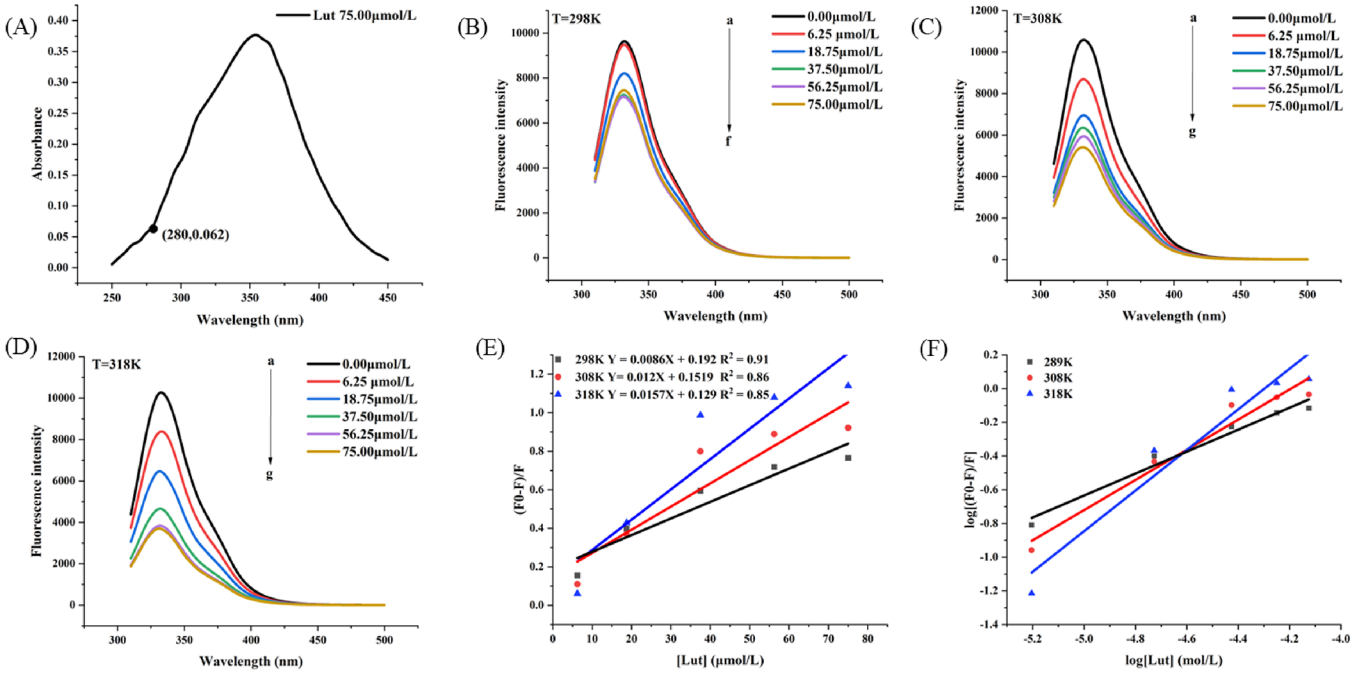

Figure 8. (A) Effect of the inner-filter effect on the fluorescence of MP. Absorbance values of the highest added concentrations are 75 μmol/L. Effect of Lut on the intrinsic fluorescence spectrum of MP at 298 K (B), 308 K (C), and 318 K (D). (E) The Stern−Volmer plots for the quenching of MP by Lut. (F) The plots for the static quenching of MP by Lut (298, 308, and 318 K). CMP = 1 mg/mL; CLut = 0 to 75 μmol/L.

of −SH groups and Tyr residues (Figure 4) in the noncovalent- and covalent-treated MP samples supported the premise that Tyr is a dominant site for the crosslinking between MP conjugates. Furthermore, the covalent samples exhibited more aggregation bands than were present in the noncovalent samples, verifying that the quinones derived from Lut oxidation can promote covalent crosslinking of proteins in alkaline conditions. This phenomenon agreed with results from the previous studies,[5,18] which reported that MP aggregates could be formed through disulfide bonds and non −S−S− linkages, and compared with the noncovalent treatment, covalent treatment increased aggregation.

PSD. The PSD of noncovalent and covalent MP−Lut samples is shown in Figure 7. The PSDs of noncovalent samples all displayed approximate multimodal distributions[45] (Figure 7A), a minor proportion of high molecular weight aggregates were observed with increasing Lut concentration, and the first small peak of samples was attributed to the monomers or oligomers in the system. Along with the Lut content increasing, the major peaks of noncovalent samples were maintained at approximately 615 nm, indicating that the noncovalent binding did not markedly change the PSD pattern and only affected the peak proportions. Multi-component distribution of MP−Lut conjugates may be due to Lut-promoted crosslinking between proteins and induced aggregate formation at different Lut concentrations. These results were consistent with those of a previous study that showed that chlorogenic acid enhanced β-lactoglobulin unfolding and aggregation.[46]

The PSDs of the covalent samples showed an approximate monomodal manner for all the fortified samples with increasing concentration of Lut. In comparison with the

https://doi.org/10.1021/acs.jafc.3c01959
J. Agric. Food Chem. 2023, 71, 9908−9921

Table 1. Binding Constants and Thermodynamic Parameters for the Interaction between MP and Lut at Different Temperatures

T (K)	regression equation	R^2	K_a (10^5 L/mol)	n	ΔH (kJ/mol)	ΔG (kJ/mol)	ΔS (kJ/mol/K)
298 K	$y = 0.76x + 3.16$	0.99	0.01	0.76	288.53	−18.00	1.03
308 K	$y = 1.11x + 4.80$	1	0.63	1.11		−28.29	
318 K	$y = 1.57x + 6.70$	0.99	99.08	1.57		−38.57	

PSDs of the noncovalent samples, the major peaks of covalent samples increased from 458 nm to approximately 615 nm with increasing Lut content, suggesting that the covalent modification had a stronger effect on the PSDs than that of noncovalent modification. The larger PSDs were consistent with the decreasing trend of surface hydrophobicity (Figure 5C). In addition, the covalent samples exhibited lower heterogeneity[47] in PSD than that seen in the noncovalent samples; therefore, the covalent samples may exhibit better solution stability, considering that the increase in the particle-specific surface area may increase water−particle interactions.[29]

Overall, the noncovalent treatment had a minor effect on the distribution of MP particle size and resulted in MP aggregation to a moderate extent, whereas covalent treatment had a relatively large impact on conjugates and considerably increased PSDs.

Fluorescence Quenching. The interaction between MP and Lut was studied by investigating the intrinsic fluorescence spectra of protein at different Lut concentrations and ambient temperatures (Figure 8). Tyr residues in MP are responsible for most of the fluorescence intensity when excited at 280 nm.[46] Since the fluorescence intensities of Tyr are sensitive to the microenvironment polarity variation, these can be used as an effective means of investigating the interaction between Lut and MP. To minimize the inner-filter effect, the absorbance at 280 nm of Lut must be <0.1.[48] According to Figure 8A, the absorption for the maximum concentration of Lut (75 μmol/L) at the excitation wavelength (280 nm) was only 0.062 (<0.1). Thus, the inner-filter effect can be excluded and further calibration fluorescence intensity is unnecessary.

Conjugating MP with an increasing concentration of Lut caused a decrease in the maximum fluorescence intensities (F_{max}) of MP at a specific ambient temperature as seen in Figure 8B (298 K), Figure 8C (308 K), and Figure 8D (318 K). The maximum emission wavelength (λ_{max}) had red-shifted to longer wavelengths by 3−5 nm, which were accompanied by slight changes in the secondary structure of noncovalent samples (Figure 5B). This suggested that the increasing Lut concentration enhanced the unfolding degree of MP and microenvironment polarity of the Tyr residues,[47] i.e., noncovalent molecular forces such as hydrogen bonds formed within the conjugates changed the structural properties of the protein and exposed more Tyr residues. A similar quenching effect has been previously reported.[46,49]

The fluorescence regression equation, the association constant (K_a), and the number of binding sites (n) of MP−Lut samples are shown in Table 1. Several quenching mechanisms can occur, including the inner-filter effect, dynamic quenching, and static quenching. If the quenching is static, the quenching constant (K_{SV}) will decrease with increasing temperature, whereas for dynamic quenching, the quenching constant will increase with increasing temperature because of the collision effect.[49] The type of fluorescence quenching mechanism of MP−Lut conjugates was analyzed using the Stern−Volmer equation (eq 2) at three different temperatures (298, 308, and 318 K). The Stern−Volmer plot showed good linearity at different temperatures (Figure 8E), suggesting that the quenching mechanism was not a mixture of the dynamic and static quenching but one of these alone. The K_{SV} values (1.15×10^3, 1.10×10^3, and 0.61×10^3 M^{-1} at 298, 308, and 318 K, respectively) decreased gradually as the temperature increased, indicating a typical static quenching induced by the formation of MP−Lut conjugates rather than collision. The bimolecular quenching rate constant (K_q) was also higher than the maximum diffusion collision quenching constant value (2.0×10^{10} L·mol^{-1}·s^{-1}), which further confirmed that the quenching type was static.[30]

For the static quenching, the K_a and n values could be calculated according to a double logarithmic equation (eq 3). The n values were all approximately equal to 1 (Table 1), suggesting that MP had a single class of binding sites for Lut under the noncovalent treatments. The K_a values (0.04×10^5, 0.57×10^5, and 15.03×10^5 M^{-1} at 298, 308, and 318 K, respectively) of MP−Lut conjugates increased with increasing temperature. This indicated that the interaction between MP and Lut could be enhanced at the higher temperature, which allowed a stronger complex formation.

The binding mode between MP and Lut was further studied using thermodynamic parameters. There are four main noncovalent forces formed between ligand and macromolecule, namely, hydrogen bonds, hydrophobic interactions, electrostatic forces, and van der Waals forces.[20] According to Ross and Subramanian[50] when $\Delta H > 0$ and $\Delta S > 0$, hydrophobic effects are the main force; when $\Delta H < 0$ and $\Delta S < 0$, van der Waals forces and hydrogen bonds play major roles in the interaction; and when $\Delta H <$ and $\Delta S > 0$, electrostatic interactions would dominate. Thermodynamic parameters were obtained using the Van't Hoff equation, and the calculated data (ΔG, ΔH, and ΔS) are shown in Table 1; the negative ΔG indicated that the complex was incorporated spontaneously.

Meanwhile, the positive value of ΔH (198.37 kJ/mol) is likely due to endothermic effects: Lut molecules approach MP particles and partly destroy the hydrophobic hydration structure in an endothermic process. Simultaneously, the positive value of ΔS (0.72 kJ/mol/K) can be attributed to the release of combined water molecules into the buffer medium, including those from the molecular pocket and hydration layer on the surface of the MP molecules;[51] as such, the water molecules in the hydration layer have a higher degree of mobility and the MPs are in a more active state.[52] Hence, the ΔH and ΔS both had positive values, indicating that hydrophobic interactions were the main forces for MP−Lut conjugates and that the binding was entropy-driven. This result is consistent with other studies, which have reported that the driving forces for the binding of flavonoids (such as kaempferol, and genistein) to β-lactoglobulin[30] and the interaction between MPs and ketones[51] were mainly hydrophobic interactions.

https://doi.org/10.1021/acs.jafc.3c01959
J. Agric. Food Chem. 2023, 71, 9908−9921

Proteomics Analysis. *Identification of Modified Proteins and Peptides.* The covalent modification of oxidized Lut toward reactive amino acid residues in MP was then analyzed via LC−MS/MS analysis. Details of the identified Lut-modified peptides and proteins present in the MP are shown in Tables 1 and 2 and Table S2. A total of 2550 modified peptides and 837 modified proteins were identified and were searched against the UniProt-Gallus gallus (Chicken) [9031]-35012-20220706.fasta. To improve the reliability, the peptide data were filtered with grafting possibility ≥95%. Thirteen Lut-modified peptides corresponding to 14 proteins were obtained.

Table 2. Distribution of Lut Modification Sites on Specific Amino Acids in MP

amino acid residues	number of adduction site
K	13
Q	6
Q/N	5
M	4
C	2
N	2
Y	1
total	33

K, Q, N, M, C, and Y represent lysine, glutamine, asparagine, methionine, cysteine, and tyrosine sites, respectively.

The 14 modified proteins from different accessions were classified on the basis of functions and locations, and 10 proteins were identified in the MP family, including chick atrial MHC, myosin motor domain-containing protein, fast MHC, actin, and myosin-binding protein C. MPs are structural proteins that are composed of myofibrils and are crucial in regulating the binding affinity.[53] Three kinds of uncharacterized proteins were found that may have resulted from the protein aggregates linked by newly formed covalent linkages. Notably, the uncharacterized proteins 1 and 2 had almost identical Lut-adducted sites (Lys884) and annotated sequences ([K]. ELEEKMVK*LVQEKNDLQLQVQAEA) as a fast MHC; therefore, uncharacterized proteins 1 and 2 may be composed of MHC isoforms. Three MPs were modified with Lut, among which the chick atrial MHC was modified with Lut at the Lys1532 site (modified peptide [K].QLDAEK*LELQAALEEAEASLEHEEGK.[I]) (Table 3).

The myosin motor domain-containing protein and myosin-binding protein C had more than one modified site and were modified with Lut at Lys1499, Glu1494, and Glu1503 (modified peptide [R]. KQ*LDAEK*LELQ*AALEEAEASLEHEEGK.[I]) and Asp544 and Lys553 (modified peptide [K].AAEN*TIVVVAGNK*VRLDVPISGEPAPTVTWK.[R]), respectively. Two subtypes of actin cytoplasmic, namely, actin cytoplasmic 1 and 2, were also identified. Actin, which constituted approximately 22% of the myofibrillar mass, was modified with Lut at Cys285 and Lys291 (modified peptide [K].C*DVDIRK*DLYANTVLSGGTTMYPGIADR. [M]). Among all proteins listed in Table 3, 14 identified proteins could form MP−Lut conjugates, of which seven were from MHC protein isoforms. This showed that myosin, as the main component of MP, accounts for 60% of the total content and had the strongest binding activity to Lut. Considering that the binding sites were mainly at the Lys sites in the amino acid sequence around 800 and 1500, Lut was more likely to bind with MP at the myosin tail.

Table 3. Lut-Modified Proteins and Peptides in Covalent MP−Lut Conjugates

accession	description	modifications	annotated sequence	positions in master proteins
Q910C5	chick atrial myosin heavy chain	1xPolyphenol [K6(100)]	[K].QLDAEKLELQAALEEAEASLEHEEGK.[I]	Q910C5 [1527−1552]
A0A1D5PFB7	myosin motor domain-containing protein			A0A1D5PFB7 [1494−1519]
A0A1D5P525	uncharacterized protein 1	1xOxidation [M6(100)]; 1xDeamidated [Q11(99)]; 1xPolyphenol [K8(99.5)]	[K].ELEEKMVKLVQEKNDLQLQVQAEADSLADAEER.[C]	A0A1D5P525 [877−909]
Q9DGM4	fast myosin heavy chain			Q9DGM4 [877−909]
Q910C5	chick atrial myosin heavy chain	2xDeamidated [Q2(100); Q11(100)]; 1xPolyphenol [K7(99.6)]	[R].KQLDAEKLELQAALEEAEASLEHEEGK.[I]	Q910C5 [1526−1552]
A0A1D5PFB7	myosin motor domain-containing protein			A0A1D5PFB7 [1493−1519]
Q9DGM5	fast myosin heavy chain	1xOxidation [M6(100)]; 1xDeamidated [Q/N]; 1xPolyphenol [K]	[K].ELEEKMVKLVQEKNDLQLQVQAEADALADAEER.[C]	Q9DGM5 [880−912]
F1P3X1	uncharacterized protein 2			F1P3X1 [878−910]
Q8JG72	fast myosin heavy chain	1xCarbamidomethyl [C1]; 1xPolyphenol [K7(99.5)]	[K].CDVDIRKDLYANTVLSGGTTMYPGIADR.[M]	Q8JG72 [880−912]
Q5ZMQ2	actin, cytoplasmic 2			Q5ZMQ2 [285−312]
P60706	actin, cytoplasmic 1			P60706 [285−312]
P16419	myosin-binding protein C, fast-type	1xDeamidated [N]; 1xPolyphenol [K13(100)]	[K].AAENTIVVVAGNKVRLDVPISGEPAPTVTWK.[R]	P16419 [541−571]
Q5F393F1NMK5	nuclear receptor coactivator uncharacterized protein 3	1xOxidation [M8(100)]; 1xDeamidated [Q11(100)]; 1xPolyphenol [K2(100)]1xPolyphenol [Y6(100)]	[R].QKPSFGPMPVQVPPPR.[G][R].KIEELYASLEK.[K]	Q5F393 [1085−1100] F1NMK5 [942−952]

https://doi.org/10.1021/acs.jafc.3c01959
J. Agric. Food Chem. 2023, 71, 9908−9921

Identification and Distribution of the Modified Sites between Lut and MP. Overall, a total of 33 modified sites were identified for the MP−Lut complex, including uncharacterized proteins. A total of 13 Lys, 6 Glu, 7 Asp, 4 Met, and 2 Cys sites as well as 1 Tyr site were modified with ratios of 39.39, 18.18, 21.21, 12.12, 6.06, and 3.03%, respectively (Table 2). These results indicated that among the MP−Lut conjugates, Lys possessed the highest reactivities, followed by Glu and Asp. Based on the peptide identification, 14 adducted sites of Lys and Tyr were clearly identified. Furthermore, 19 modified sites formed through other modifications such as oxidation (Met), deamidation (Glu), and carbamidomethylation (Cys). Cys and Met are the most easily oxidizable amino acids since they contain sulfur atoms, whose anion is a strong nucleophile rich in electrons allowing them to act as antioxidants. Other amino acids such as Tyr, Try, His, Arg, and Lys have been highlighted as highly susceptible to free radicals.[54] The substances that reacted with the above sites might be the unidentified polymer of Lut or the oxidation of MP itself. The covalent bonds formed between Cys/Tyr and Lut would decrease the content of tested sulfhydryl/Tyr residues, which was consistent with our earlier results (Figure 4). Therefore, Cys and other amino acid residues may be the sites used for adduction. Peptides containing alkali amino acids are deeply embedded inside proteins and rarely participate in the adduction process because of steric hindrance;[55] therefore, the crosslinking between the internal Cys residues and Lut in this study may be inhibited by the steric effect, exhibiting a lower degree of modification than predicted.

The Influence of Lut Concentration on Peptides and Modified Sites. We identified 57 unique peptides at the low Lut concentration, 41 unique peptides at the medium Lut concentration, and 13 unique peptides at the high Lut concentration, as seen in the Venn comparison chart (Figure 9) and Table 3. The number of modified peptides gradually decreased with the increasing Lut concentration. The type of modified proteins was unaffected by the Lut concentration, as indicated by the unchanged protein source of the modified peptides for all the Lut concentration groups, whereas the category of modified peptides and the modified sites were Lut concentration-dependent. Specifically, Lys, Gln, Met, and Asn were modified in the peptides for the low Lut concentration groups, whereas Lys and Asn were modified in the medium Lut concentration groups and Lys was modified in the high Lut concentration groups. The type of unique modified peptides and sites decreased progressively with the increasing Lut concentration, which may be related to the aggregation of the conjugates at high concentrations. Although the difference mainly lay in the type of peptide, the abundance of peptides affected by the Lut concentration was low compared with the total peptide number and the overall impact on binding efficiency might not play a decisive role. Significantly, when amino acid side chains from different unique peptides are modified by reactive oxygen species, the metabolism of those amino acids will also likely be altered.[54]

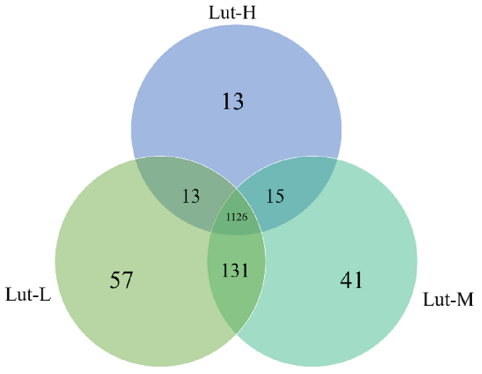

Figure 9. Venn diagram of peptide distribution at different Lut concentrations. Lut-L, Lut-M, and Lut-H represent the low, medium, and high, concentrations of Lut-modified MP upon covalent treatments.

Antioxidant Properties. Construction of MP−polyphenol conjugates can improve the antioxidant properties of complexes. The introduction of hydroxyl groups from the polyphenols can enhance antioxidant activities, and the number of hydroxyl groups in the polyphenol ring is recognized as being positively correlated with antioxidant ability.[25] The influence of binding on the antioxidant properties of MP−Lut conjugates under different concentration and various thermal treatments was analyzed by a combination of DPPH, ABTS, and Fe^{2+} reducing power (Figure 10).

All samples showed dose-dependent DPPH radical scavenging capacity at 0−120 μmol Lut/g protein (Figure 10A). The DPPH radical scavenging capacities of low-, medium-, and high-concentration MP−Lut conjugates were significantly improved ($P < 0.05$) by 6.08, 27.71, and 36.86% (noncovalent treatments) and 7.34, 14.20, and 35.99% (covalent treatments) compared with those of the control MP at 25 °C. Similar reports showed that the modification of epicatechin[19] and catechins[25] on MP conjugates enhanced the DPPH scavenging ability. We found that after thermal treatment, the DPPH radical scavenging activities of both noncovalent and covalent samples decreased slightly with the increase in temperature. Notably, the noncovalent samples showed stronger thermal stability of the DPPH radical scavenging capacity than that of covalent samples at the medium Lut concentration; this phenomenon might be due to the structural change and aggregation of the MPs caused by *o*-quinone (catechol-containing Lut) as crosslinker-mediated protein crosslinking, which may have changed the electrical environment of the Lut molecule and diminished the capacity of the phenolic hydroxyl groups to donate hydrogen or electrons.[46]

The ABTS scavenging activities of the MP−Lut conjugates (Figure 10B) were approximately consistent with the DPPH free radical scavenging activities. The ABTS scavenging activities of MP conjugates increased with increasing Lut concentration (low, medium, and high) by 7.60, 14.06, and 35.74%, respectively, in noncovalent treatments and by 3.32, 10.63, and 30.95%, respectively, in covalent treatments as compared with those in the control group. The ABTS scavenging activity of the noncovalent samples showed stronger thermal stability than that of the covalent group, especially at low and medium concentrations. After thermal treatment at 75 °C, the ABTS scavenging activity of noncovalent samples was significantly ($P < 0.05$) higher than that of covalent ones at low concentrations (Figure 10B). Considering that the ABTS scavenging activity of chlorogenic acid-modified β-lactoglobulin[46] also remained relatively stable under thermal treatment at 85 °C, thermal treatments may not initiate further oxidation of the complex.

The values of Fe^{2+} reducing power upon different binding ways remained almost equivalent at different concentrations.

https://doi.org/10.1021/acs.jafc.3c01959
J. Agric. Food Chem. 2023, 71, 9908−9921

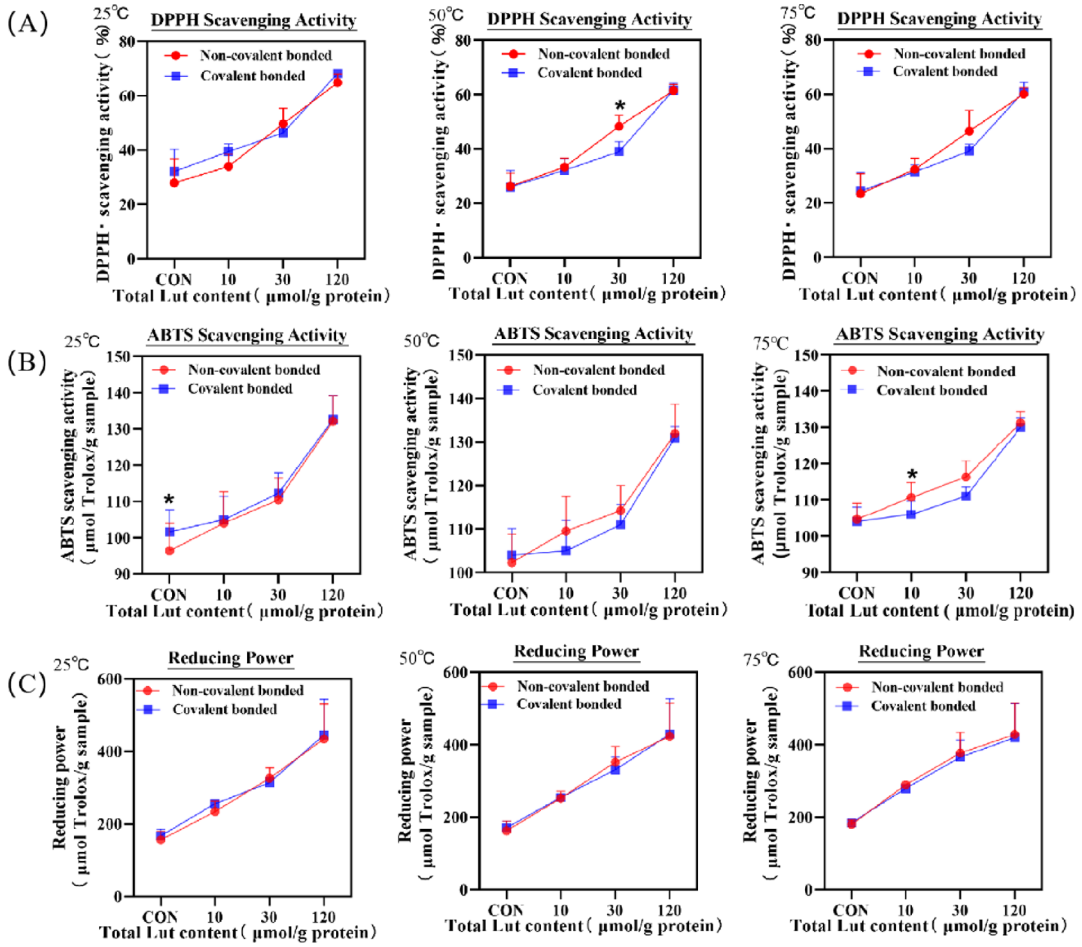

Figure 10. Antioxidant activities of MP following different treatments in terms of (A) scavenging capacity on 2,2-diphenyl-1-picrylhydrazyl radicals, (B) ABTS scavenging ability, and (C) reducing power. *$p < 0.05$, **$p < 0.01$, ***$p < 0.001$ were compared between the noncovalent and covalent groups.

The Fe^{2+} reducing power values of low-, medium-, and high-concentration MP−Lut conjugates improved significantly ($P < 0.05$) by 60.56, 109.44, and 137.87% (noncovalent treatments) and 51.35, 97.92, and 127.06% (covalent treatments) as compared with that of the control MP at 25 °C. With the increase in thermal treatment temperature, the reducing power of all the noncovalent/covalent samples showed no conspicuous changes. These mutually supporting results confirmed that the binding method, either noncovalent or covalent, had only a minor effect on the antioxidant properties of MP−Lut samples, whereas the binding amount of Lut played a predominant role. Similarly, digestive results of a phosvitin and the gallic acid complex[56] showed that noncovalent complexes had greater antioxidant and polyphenol protective effects than that of the covalent complexes. In summary, the content of Lut primarily determined the antioxidant capacity of the MP−Lut conjugates, which was dramatically improved compared with that of the control group at higher concentrations of Lut. The binding modes and preparation ways had minimal effect on the antioxidant activity, and each group had unimpaired antioxidant ability under thermal conditions, indicating that the complex can be used as an additive in heat-treated food. Although the stability of flavonoids was relatively poor, the antioxidant activity of flavonoids would not be affected at pH 9.0. Given the similar antioxidant activity obtained from the two binding methods, noncovalent modification ways with simpler operations would be preferentially selected to prepare the complex.

In conclusion, this study explored the difference between MP−Lut conjugates fabricated through noncovalent and covalent modification. Upon covalent treatment, Lut was successfully conjugated with MP through binding with Cys, Tyr, and Tyr (Figures 4 and 8). The Tyr−Tyr and S−S bonds via the Lut redox reaction were the predominant driving force for MP aggregate formation at low concentrations of Lut, whereas at high concentrations, the bonding involved in protein aggregation was governed by Lut-bridged crosslinking (Figures 2 and 6). The hydrophobic interactions were the main forces for noncovalent MP−Lut conjugates, and the binding was entropy-driven (Table 1). The antioxidant property of MP−Lut conjugates was enhanced as expected but was barely affected by the conjugation method used. The binding amount of Lut determined the strength of the antioxidant property, which indicated that (1) the in vitro antioxidant activity of MP−Lut conjugates may not be related to the binding mode but was only dependent on the content of Lut and (2) the bioactivity of Lut in the protein complex was not affected by transient alkaline and thermal treatment. Furthermore, the noncovalent samples showed greater thermal stability since the antioxidant ability for noncovalent groups was slightly improved relative to that of covalent samples during the heating treatment. This means that the simpler

https://doi.org/10.1021/acs.jafc.3c01959
J. Agric. Food Chem. 2023, 71, 9908−9921

noncovalent method can produce equally effective results without chemical reagent addition or exhaustive labor. This finding provides valuable insights into the interaction between MP and Lut and its effects on the structure and function of MP, as well as the antioxidant effects of Lut during thermal processing. Furthermore, our study provides information on how to maintain the health benefits of Lut, which is used for industrial production in muscle protein-rich products and other foods, by using simpler food processing conditions.

■ ASSOCIATED CONTENT

Supporting Information

The Supporting Information is available free of charge at https://pubs.acs.org/doi/10.1021/acs.jafc.3c01959.

Characterization of the content of amino acid side-chain group changes of the untreated MP, noncovalent/covalent MP−Lut conjugates (Table S1); peptide modification identification table of the covalent MP−Lut conjugates (Table S2) (PDF)

■ AUTHOR INFORMATION

Corresponding Authors

Xue Zhao − *State Key Laboratory of Meat Quality Control and Cultured Meat Development; Jiangsu Collaborative Innovation Center of Meat Production and Processing, Quality and Safety Control, Nanjing Agricultural University, Nanjing 210095, PR China;* orcid.org/0000-0003-3111-9648; Email: zhaoxue@njau.edu.cn

Xinglian Xu − *State Key Laboratory of Meat Quality Control and Cultured Meat Development; Jiangsu Collaborative Innovation Center of Meat Production and Processing, Quality and Safety Control, Nanjing Agricultural University, Nanjing 210095, PR China;* orcid.org/0000-0003-4507-3214; Email: xlxus@njau.edu.cn

Author

Zhenyang Wu − *State Key Laboratory of Meat Quality Control and Cultured Meat Development; Jiangsu Collaborative Innovation Center of Meat Production and Processing, Quality and Safety Control, Nanjing Agricultural University, Nanjing 210095, PR China*

Complete contact information is available at: https://pubs.acs.org/10.1021/acs.jafc.3c01959

Author Contributions

Z.W.: formal analysis, investigation, and writing—original draft. X.Z.: conceptualization, methodology, software, supervision, and writing—review and editing. X.X.: validation, supervision, and writing—review and editing.

Funding

This work was supported by the Natural Science Foundation of Jiangsu Province of China (BK20210405), National Natural Science Foundation of China (Grant No. 31972097), the Fundamental Research Funds for the Central Universities (KYQN2022002), and the Priority Academic Program Development of Jiangsu Higher Education Institution (PAPD).

Notes

The authors declare no competing financial interest.

■ REFERENCES

(1) Xu, Y.; Xu, X. Modification of myofibrillar protein functional properties prepared by various strategies: A comprehensive review. *Compr. Rev. Food Sci. Food Saf.* **2021**, *20*, 458−500.

(2) Cao, Y.; Ai, N.; True, A. D.; Xiong, Y. L. Effects of (−)-Epigallocatechin-3-Gallate incorporation on the physicochemical and oxidative stability of myofibrillar protein−soybean oil emulsions. *Food Chem.* **2018**, *245*, 439−445.

(3) Maqsood, S.; Benjakul, S.; Shahidi, F. Emerging role of phenolic compounds as natural food additives in fish and fish products. *Crit. Rev. Food Sci. Nutr.* **2013**, *53*, 162−179.

(4) Xu, Q.-D.; Yu, Z.-L.; Zeng, W.-C. Structural and functional modifications of myofibrillar protein by natural phenolic compounds and their application in pork meatball. *Food Res. Int.* **2021**, *148*, No. 110593.

(5) Guo, A.; Jiang, J.; True, A. D.; Xiong, Y. L. Myofibrillar protein cross-linking and gelling behavior modified by structurally relevant phenolic compounds. *J. Agric. Food Chem.* **2021**, *69*, 1308−1317.

(6) Bhullar, K. S.; Rupasinghe, H. P. V. Polyphenols: Multipotent therapeutic agents in neurodegenerative diseases. *Oxid. Med. Cell. Longevity* **2013**, *2013*, No. 891748.

(7) Hayasaka, N.; Shimizu, N.; Komoda, T.; Mohri, S.; Tsushida, T.; Eitsuka, T.; Miyazawa, T.; Nakagawa, K. Absorption and metabolism of luteolin in rats and humans in relation to in vitro anti-inflammatory effects. *J. Agric. Food Chem.* **2018**, *66*, 11320−11329.

(8) Cao, Y.; Xiong, Y. L. Interaction of whey proteins with phenolic derivatives under neutral and acidic pH conditions. *J. Food Sci.* **2017**, *82*, 409−419.

(9) Guo, A.; Xiong, Y. L. Glucose oxidase promotes gallic acid-myofibrillar protein interaction and thermal gelation. *Food Chem.* **2019**, *293*, 529−536.

(10) Wang, X.; Zhang, J.; Lei, F.; Liang, C.; Yuan, F.; Gao, Y. Covalent complexation and functional evaluation of (−)-Epigallocatechin Gallate and α-Lactalbumin. *Food Chem.* **2014**, *150*, 341−347.

(11) Yi, J.; Ning, J.; Zhu, Z.; Cui, L.; Decker, E. A.; McClements, D. J. Impact of interfacial composition on co-oxidation of lipids and proteins in oil-in-water emulsions: Competitive displacement of casein by surfactants. *Food Hydrocolloids* **2019**, *87*, 20−28.

(12) Wang, S.; Yang, J.; Shao, G.; Liu, J.; Wang, J.; Yang, L.; Li, J.; Liu, H.; Zhu, D.; Li, Y.; Jiang, L. PH-induced conformational changes and interfacial dilatational rheology of soy protein isolated/soy hull polysaccharide complex and its effects on emulsion stabilization. *Food Hydrocolloids* **2020**, *109*, No. 106075.

(13) Shahzad, F.; Abdullah; Hui, Z.; Jochen, W. A comprehensive review on polarity, partitioning, and interactions of phenolic antioxidants at oil-water interface of food emulsions. *Compr. Rev. Food Sci. Food Saf.* **2021**, *20*, 4250−4277.

(14) Imran, M.; Rauf, A.; Abu-Izneid, T.; Nadeem, M.; Shariati, M. A.; Khan, I. A.; Imran, A.; Orhan, I. E.; Rizwan, M.; Atif, M.; Gondal, T. A.; Mubarak, M. S. Luteolin, a flavonoid, as an anticancer agent: A review. *Biomed. Pharmacother.* **2019**, *112*, No. 108612.

(15) Kroll, J.; Rawel, H. M.; Rohn, S. Reactions of plant phenolics with food proteins and enzymes under special consideration of covalent bonds. *Food Sci. Technol. Res.* **2003**, *9*, 205−218.

(16) Hu, Y.; Liu, F.; Pang, J.; McClements, D. J.; Zhou, Z.; Li, B.; Li, Y. Biopolymer additives enhance tangeretin bioavailability in emulsion-based delivery systems: An in vitro and in vivo study. *J. Agric. Food Chem.* **2021**, *69*, 730−740.

(17) Miyashita, A.; Ito, J.; Parida, I. S.; Syoji, N.; Fujii, T.; Takahashi, H.; Nakagawa, K. Improving water dispersibility and bioavailability of luteolin using microemulsion system. *Sci. Rep.* **2022**, *12*, 11949.

(18) Chen, K.; Chen, X.; Liang, L.; Xu, X. Gallic acid-aided cross-linking of myofibrillar protein fabricated soluble aggregates for enhanced thermal stability and a tunable colloidal state. *J. Agric. Food Chem.* **2020**, *68*, 11535−11544.

(19) Chen, J.; Zhang, X.; Chen, X.; Pius Bassey, A.; Zhou, G.; Xu, X. Phenolic modification of myofibrillar protein enhanced by ultrasound: The structure of phenol matters. *Food Chem.* **2022**, *386*, No. 132662.

(20) Guo, A.; Xiong, Y. L. Myoprotein-phytophenol interaction: Implications for muscle food structure-forming properties. *Compr. Rev. Food Sci. Food Saf.* **2021**, *20*, 2801−2824.
(21) Liu, J.; Yong, H.; Yao, X.; Hu, H.; Yun, D.; Xiao, L. Recent advances in phenolic−protein conjugates: synthesis, characterization, biological activities and potential applications. *RSC Adv.* **2019**, *9*, 35825.
(22) Han, M.; Zhang, Y.; Fei, Y.; Xu, X.; Zhou, G. Effect of microbial transglutaminase on NMR relaxometry and microstructure of pork myofibrillar protein gel. *Eur. Food Res. Technol.* **2009**, *228*, 665−670.
(23) Ali, M.; Keppler, J. K.; Coenye, T.; Schwarz, K. Covalent whey protein-rosmarinic acid interactions: A comparison of alkaline and enzymatic modifications on physicochemical, antioxidative, and antibacterial properties. *J. Food Sci.* **2018**, *83*, 2092−2100.
(24) Winters, A. L.; Minchin, F. R. Modification of the lowry assay to measure proteins and phenols in covalently bound complexes. *Anal. Biochem.* **2005**, *346*, 43−48.
(25) Xu, Y.; Han, M.; Huang, M.; Xu, X. Enhanced heat stability and antioxidant activity of myofibrillar protein-dextran conjugate by the covalent adduction of polyphenols. *Food Chem.* **2021**, *352*, No. 129376.
(26) Benjakul, S.; Morrissey, M. T. Protein hydrolysates from pacific whiting solid wastes. *J. Agric. Food Chem.* **1997**, *45*, 3423−3430.
(27) Liu, F.; Sun, C.; Yang, W.; Yuan, F.; Gao, Y. Structural characterization and functional evaluation of lactoferrin−polyphenol conjugates formed by free-radical graft copolymerization. *RSC Adv.* **2015**, *5*, 15641−15651.
(28) Alizadeh-Pasdar, N.; Li-Chan, E. C. Y. Comparison of protein surface hydrophobicity measured at various pH values using three different fluorescent probes. *J. Agric. Food Chem.* **2000**, *48*, 328−334.
(29) Chen, X.; Xu, X.; Zhou, G. Potential of high pressure homogenization to solubilize chicken breast myofibrillar proteins in water. *Innovative Food Sci. Emerging Technol.* **2016**, *33*, 170−179.
(30) Li, T.; Hu, P.; Dai, T.; Li, P.; Ye, X.; Chen, J.; Liu, C. Comparing the binding interaction between β-Lactoglobulin and flavonoids with different structure by multi-spectroscopy analysis and molecular docking. *Spectrochim. Acta, Part A* **2018**, *201*, 197−206.
(31) Siddhuraju, P. The antioxidant activity and free radical-scavenging capacity of phenolics of raw and dry heated moth bean (*vigna aconitifolia*) (Jacq.) marechal seed extracts. *Food Chem.* **2006**, *99*, 149−157.
(32) Yildirim-Elikoglu, S.; Erdem, Y. K. Interactions between milk proteins and polyphenols: binding mechanisms, related changes, and the future trends in the dairy industry. *Food Rev. Int.* **2018**, *34*, 665−697.
(33) Rohn, S. Possibilities and limitations in the analysis of covalent interactions between phenolic compounds and proteins. *Food Res. Int.* **2014**, *65*, 13−19.
(34) Cao, Y.; Xiong, Y. L. Binding of gallic acid and epigallocatechin gallate to heat-unfolded whey proteins at neutral pH alters radical scavenging activity of in vitro protein digests. *J. Agric. Food Chem.* **2017**, *65*, 8443−8450.
(35) Feng, G.; Han, K.; Yang, Q.; Feng, W.; Guo, J.; Wang, J.; Yang, X. Interaction of pyrogallol-containing polyphenols with mucin reinforces intestinal mucus barrier properties. *J. Agric. Food Chem.* **2022**, *70*, 9536−9546.
(36) Le Bourvellec, C.; Renard, C. M. G. C. Interactions between polyphenols and macromolecules: Quantification methods and mechanisms. *Crit. Rev. Food Sci. Nutr.* **2012**, *52*, 213−248.
(37) Guyon, C.; Meynier, A.; de Lamballerie, M. Protein and lipid oxidation in meat: A review with emphasis on high-pressure treatments. *Trends Food Sci. Tech.* **2016**, *50*, 131−143.
(38) King, L.; Lehrer, S. S. Thermal unfolding of myosin rod and light meromyosin: Circular dichroism and tryptophan fluorescence studies. *Biochemistry* **1989**, *28*, 3498−3502.
(39) Cao, Y.; Xiong, Y. L. Chlorogenic acid-mediated gel formation of oxidatively stressed myofibrillar protein. *Food Chem.* **2015**, *180*, 235−243.
(40) Li, L.; Zhao, X.; Xu, X. Trace the difference driven by unfolding-refolding pathway of myofibrillar protein: Emphasizing the changes on structural and emulsion properties. *Food Chem.* **2022**, *367*, No. 130688.
(41) Wang, Y.; Zhang, L.; Wang, P.; Xu, X.; Zhou, G. PH-shifting encapsulation of curcumin in egg white protein isolate for improved dispersity, antioxidant capacity and thermal stability. *Food Res. Int.* **2020**, *137*, No. 109366.
(42) Jia, J.; Gao, X.; Hao, M.; Tang, L. Comparison of binding interaction between β-Lactoglobulin and three common polyphenols using multi-spectroscopy and modeling methods. *Food Chem.* **2017**, *228*, 143−151.
(43) Aewsiri, T.; Benjakul, S.; Visessanguan, W.; Eun, J.-B.; Wierenga, P. A.; Gruppen, H. Antioxidative activity and emulsifying properties of cuttlefish skin gelatin modified by oxidised phenolic compounds. *Food Chem.* **2009**, *117*, 160−168.
(44) Domínguez, R.; Pateiro, M.; Munekata, P. E. S.; Zhang, W.; Garcia-Oliveira, P.; Carpena, M.; Prieto, M. A.; Bohrer, B.; Lorenzo, J. M. Protein oxidation in muscle foods: A comprehensive review. *Antioxidants* **2022**, *11*, 60.
(45) Xu, Y.; Zhao, Y.; Wei, Z.; Zhang, H.; Dong, M.; Huang, M.; Han, M.; Xu, X.; Zhou, G. Modification of myofibrillar protein via glycation: Physicochemical characterization, rheological behavior and solubility property. *Food Hydrocolloids* **2020**, *105*, No. 105852.
(46) Qie, X.; Chen, W.; Zeng, M.; Wang, Z.; Chen, J.; Goff, H. D.; He, Z. Interaction between β-Lactoglobulin and chlorogenic acid and its effect on antioxidant activity and thermal stability. *Food Hydrocolloids* **2021**, *121*, No. 107059.
(47) Boachie, R. T.; Okagu, O. D.; Abioye, R.; Hüttmann, N.; Oliviero, T.; Capuano, E.; Fogliano, V.; Udenigwe, C. C. Lentil protein and tannic acid interaction limits in vitro peptic hydrolysis and alters peptidomic profiles of the proteins. *J. Agric. Food Chem.* **2022**, *70*, 6519−6529.
(48) van de Weert, M. Fluorescence quenching to study protein-ligand binding: Common errors. *J. Fluoresc.* **2010**, *20*, 625−629.
(49) Dai, T.; Chen, J.; Li, Q.; Li, P.; Hu, P.; Liu, C.; Li, T. Investigation the interaction between procyanidin dimer and α-Amylase: Spectroscopic analyses and molecular docking simulation. *Int. J. Biol. Macromol.* **2018**, *113*, 427−433.
(50) Ross, P. D.; Subramanian, S. Thermodynamics of protein association reactions: Forces contributing to stability. *Biochemistry* **1981**, *20*, 3096−3102.
(51) Wang, H.; Zhang, H.; Liu, Q.; Xia, X.; Chen, Q.; Kong, B. Exploration of interaction between porcine myofibrillar proteins and selected ketones by GC-MS, multiple spectroscopy, and molecular docking approaches. *Food Res. Int.* **2022**, *160*, No. 111624.
(52) Pal, S. K.; Peon, J.; Zewail, A. H. Ultrafast surface hydration dynamics and expression of protein functionality: α-Chymotrypsin. *Proc. Natl. Acad. Sci.* **2002**, 15297.
(53) Tang, C.; Zhang, W.; Wang, Y.; Xing, L.; Xu, X.; Zhou, G. Identification of rosmarinic acid-adducted sites in meat proteins in a gel model under oxidative stress by triple TOF MS/MS. *J. Agric. Food Chem.* **2016**, *64*, 6466−6476.
(54) Xiong, Y. L.; Guo, A. Animal and plant protein oxidation: Chemical and functional property significance. *Foods* **2021**, *10*, 40.
(55) Jia, Y.; Yan, X.; Li, X.; Zhang, S.; Huang, Y.; Zhang, D.; Li, Y.; Qi, B. Soy protein−phlorizin conjugate prepared by tyrosinase catalysis: Identification of covalent binding sites and alterations in protein structure and functionality. *Food Chem.* **2023**, *404*, No. 134610.
(56) Jiang, B.; Zhong, S.; Yu, H.; Chen, P.; Li, B.; Li, D.; Liu, C.; Feng, Z. Covalent and noncovalent complexation of phosvitin and gallic acid: Effects on protein functionality and in vitro digestion properties. *J. Agric. Food Chem.* **2022**, *70*, 11715−11726.

https://doi.org/10.1021/acs.jafc.3c01959
J. Agric. Food Chem. 2023, 71, 9908−9921